Plasma Injectors Based on Rotating Gliding Discharge with Reverse Vortex Flow with Liquid Electrode

Fedirchyk I.[1], Nedybaliuk O.[1], Chernyak V.[1], Liptuga A.[2]

[1]*Taras Shevchenko National University of Kyiv, 64/13, Volodymyrska Street, 01601, Kyiv, Ukraine, e-mail: igor.fedirchyk@univ.net.ua*

[2]*V. Lashkaryov Institute of Semiconductor Physics, National Academy of Sciences of Ukraine, 41, pr. Nauki, 03028, Kyiv, Ukraine*

The researched plasma-liquid system was developed to create discharge that is compliant with industrial requirements. Current-voltage characteristics of discharge and their dependence on interelectrode distance are obtained. The main components of plasma are presented based on spectroscopy results. Measured electron, vibrational and rotational temperatures prove that system is able to generate non-equilibrium discharge plasma at atmospheric pressure without severe electrode erosion.

Keywords: plasma catalysis, rotating gliding discharge, plasma injector, liquid electrode

1 INTRODUCTION

The energy efficiency is an important parameter that defines the range of possible applications for plasma-chemical technology. The problems with energy efficiency stem from the fact that plasma is commonly generated by using electricity, which is the most expensive type of energy produced in energy industry. Therefore, one of the most efficient ways for plasma-chemistry to reach industrial viability is to combine it with traditional chemical technologies. This type of inclusion is possible only if the effective method for the injection of plasma into the reaction chamber is provided. In addition, the effective control of chemical reactions via plasma is only possible when it is used as a catalyst. Apart from the problem of efficiency, the widespread industrial use of plasma is obstructed by the high erosion rate of metal electrodes.

A number of different arc discharges are used for plasma generation at atmospheric pressure, including transverse arc [1], gliding arc [2-5] and rotating gliding arc [6-12]. Comparing to gliding arc [2-5], transverse arc [1] has fixed length of discharge column and shorter service time. The rotating gliding arcs [6-12] subdivide based on the presence [6-9] or absence [10-12] of the longitudinal motion of discharge column. Rotating gliding arcs featuring longitudinal motion [6-9] are not sufficiently stable for continuous use. Stability of high-pressure discharge in powerful plasma generators is achieved by the inclusion of vortex gas flow [13]. The rotating gliding arc without longitudinal motion has fixed discharge column, in comparison to gliding arc with longitudinal motion [2-9], and longer lifetime than transverse arc [1]. In low-powered high-pressure discharges, the "tornado"-type reverse vortex flow can be used for the spatial stabilization of plasma channel [14] and injected plasma torch.

Plasma-liquid system with "tornado"-type reverse vortex flow and liquid electrode, in which distilled water is used as a working liquid, can provide a solution to the problems of energy efficiency and electrode erosion; recently this type of systems saw an extensive amount of research [15,16]. In such systems, the destruction of liquid electrode is prevented by maintaining the level of liquid through continuous replenishment via injection pumps. The activation of water produces hydroxyl, atomic oxygen and atomic hydrogen, significantly increasing the rates of chemical reactions as a result.

2 EXPERIMENTAL SETUP

The experimental setup (shown at Fig.1) consists of plasma-liquid system based on rotating gliding discharge with liquid electrode. The discharge scheme was reviewed in more detail in previous publication [15]. Discharge system consists of cylindrical quartz chamber, which is sealed from both sides with stainless steel flanges. A T-shaped cylindrical electrode is inserted into the centre of bottom flange. The top flange has an opening with copper sleeve inserted inside. Quartz chamber is filled with

distilled water; amount of liquid can be maintained at a required level by the injection pump through a water input aperture.

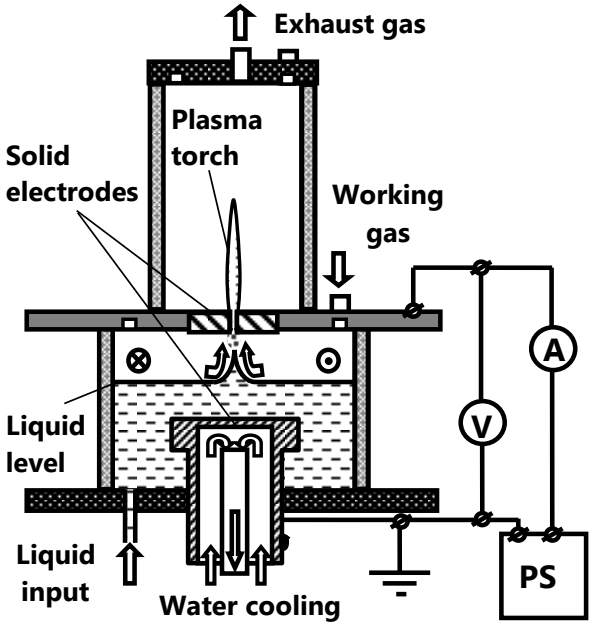

Fig.1: Scheme of experimental setup in LC mode

Gas is injected into the system through the inlets carved in the upper flange. The gas flow is directed tangentially to the wall of the quartz tube, which results in the creation of "tornado"-type reverse vortex gas flow that travels along the surface of liquid towards quartz cylinder axis and exits it through the opening in the copper sleeve. Discharge generates a plasma channel, one end of which is located on the surface of the sleeve; the other end is located on the surface of a liquid. The reverse vortex gas flow causes the rotation of the plasma channel around the system axis and its expulsion from the aperture in the upper flange sleeve. The end of the plasma channel, which is connected to a solid electrode, glides along the surface of the sleeve during rotation. The voltage between electrodes is provided by a DC power supply and can reach up to 7 kV. Discharge has two modes of operation depending on what electrode is used as a cathode: bottom electrode in case of liquid cathode (LC) mode and top electrode in case of solid cathode (SC) mode. The anode was grounded and high voltage was supplied to the cathode during the experiments. The behaviour of the discharge during liquid cathode and solid cathode modes was captured by a video camera. The parameters of the discharge were obtained from the analysis of its current-voltage characteristics. Collected data was used to study the dependence of discharge parameters on the distance between solid and liquid electrodes. The main diagnostics of plasma was conducted via emission spectroscopy. Emission spectra were registered on a spectral device, which consists of an optical fibre and a calibrated S-150-2-3648 USB spectrometer that allows for the registration of spectral lines in the wavelength range from 200 nm to 1000 nm with the resolution of less than 0.13 nm/pixel. Electron temperature T_e^* of atomic hydrogen H was obtained by analysing relative integral intensities of H_α (656.3 nm) and H_β (486.1 nm) lines. Electron temperature of atomic oxygen was calculated via Boltzmann diagrams based on the three most intensive multiplets of oxygen (777.2, 844.6, and 926.6 nm). Rotational T_r^* and vibrational T_v^* temperatures of hydroxyl and nitrogen were obtained by comparing experimental emission spectra with those calculated by SPECAIR [17] modelling software by using previously known electron temperature of atomic oxygen O.

3 RESULTS AND DISCUSSION

Fig.2 shows the difference between discharge behaviour in LC and SC modes. The volume of visible discharge channel is larger in case of LC mode. Calculated values of effective discharge current density are approximately 0.22 A/cm^2 for LC mode and 0.77 A/cm^2 for SC mode, which are less than required to classify the discharge as an electric arc. Discharge properties were measured for the 18, 22 and 27 mm distance between top and bottom solid electrodes.

Fig.3 shows the dependence of discharge power on the distance between solid and liquid electrodes during SC operation mode. The gap distance between liquid electrode and upper flange was regulated in range from 3 mm to the distance between solid electrodes (22 mm). Fig.3 shows that the increase of interelectrode distance leads to unmonotonous voltage and power increase. However, when the thickness of liquid layer over the bottom solid electrode reaches some minimal value,

the plasma channel pushes liquid apart and discharge transitions into the traditional arc between two solid electrodes. The influence of liquid on the properties of discharge diminishes and it no longer causes the additional voltage drop, resulting in the sharp decrease of the discharge power.

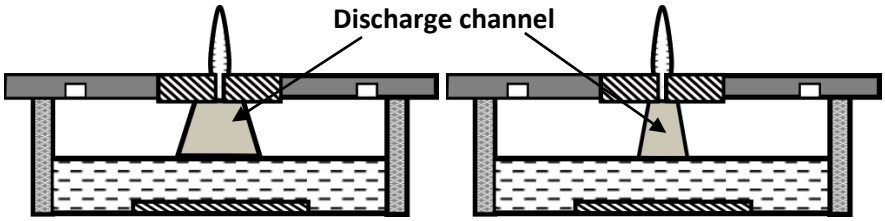

Fig.2: Schemes showing discharge channel behaviour in LC (left panel) and SC (right panel) modes

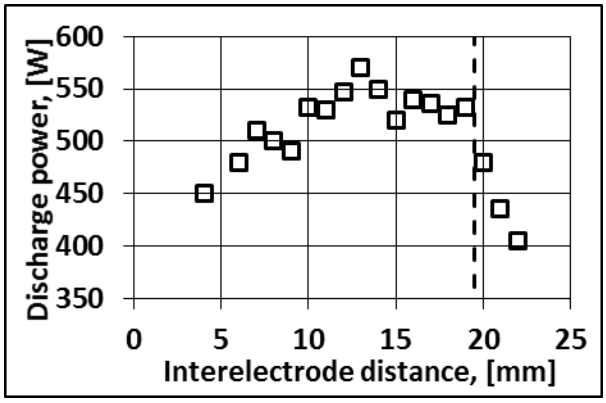

Fig.3: Dependence of discharge power on distance between solid and liquid electrodes during SC mode. Electrical current was 300 mA. Distance between metal electrodes was 22 mm. Dashed line marks the approximate point of discharge regime transition which was obtained from video analysis

According to emission spectra, the main components of plasma generated in discharge gap are OH, H and O, which are the active species that initiate chemical chain reactions. In addition, spectra contain the bands of N_2, which originates from the working gas (air) and is mostly inert. Fig.4 presents the comparison between the emission spectrum of plasma measured during the experiment and the spectrum calculated for OH species in SPECAIR modelling software based on the electron temperature calculations for atomic oxygen. High similarity between spectra allows for the assumption that plasma species have the same parameters as those set in the simulation; therefore, the vibrational and rotational temperatures of plasma species were taken from the model.

The electron temperatures T_e^* of atomic hydrogen and oxygen and the rotational T_r^* and vibrational T_v^* temperatures of hydroxyl and nitrogen were calculated from the emission spectra of plasma. In discharge gap plasma, rotational and vibrational temperatures of OH component have the same value $T_v^*(OH) = T_r^*(OH) = 4100 \pm 200$ K. This can be caused by the specific gas flow direction near the water surface, which is parallel to the plasma channel and electric current flow. The electron temperatures of H and O components have different values: $T_e^*(H) = 3200 \pm 500$ K and $T_e^*(O) = 5000 \pm 500$ K. Plasma in the torch became non-isothermal immediately after its expulsion from the discharge area. The vibrational and rotational temperatures of species in plasma torch substantially differentiate at the distance of 5 mm over the upper flange: in the case of OH $T_v^*(OH) = 4200 \pm 200$ K and $T_r^*(OH) = 3200 \pm 200$ K, in the case of N_2 $T_v^*(N_2) = 5000 \pm 200$ K and $T_r^*(N_2) = 3500 \pm 200$ K. The difference in temperatures can be attributed to the appearance of gas flow direction component that is lateral to plasma channel. Plasma torch is effectively injected on the distance of 150 mm into reaction chamber. The electron temperatures of H and O components in the torch are $Te^*(H) = 3500 \pm 500$ K and $Te^*(O) = 5200 \pm 500$ K. The difference between electron temperatures Te*(H) and Te*(O) requires additional future investigations.

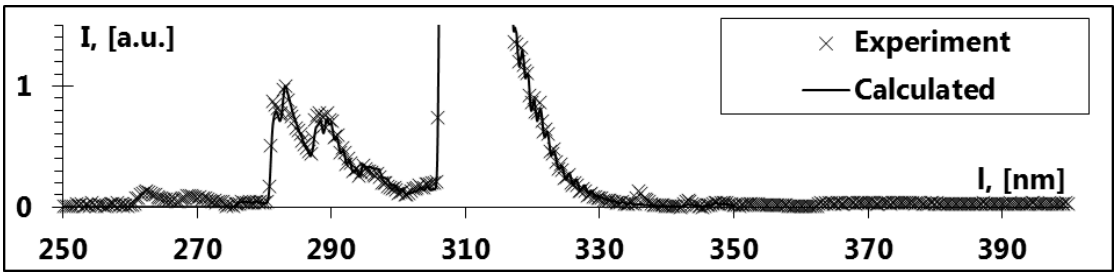

Fig.4: Comparison between experimental and calculated emission spectra of plasma

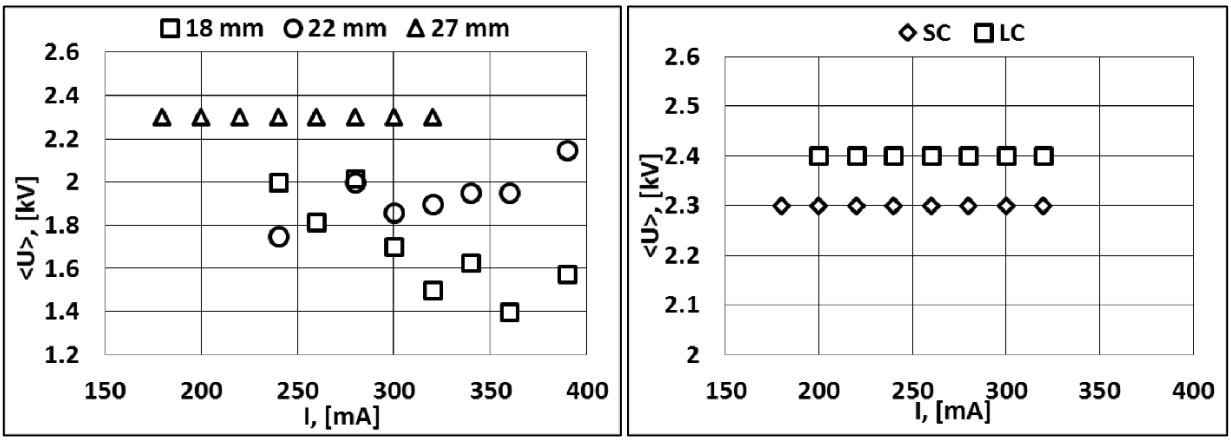

Fig.5: CVCs of rotating gliding discharge: in SC mode for different distances between solid electrodes (left panel) and for SC and LC modes at 27 mm distance between solid electrodes (right panel)

Fig.5 shows the current-voltage characteristics (CVC) of rotating gliding discharge in SC mode and at different distances between solid electrodes. The decrease of CVC in case of 18 mm distance between solid electrodes can be explained by the intense production of bubbles caused by an electrolysis in the thin layer of water, which provides better conditions for the discharge.

4 CONCLUSIONS

The plasma-liquid system based on rotating gliding discharge with "tornado"-type reverse vortex flow with one liquid electrode was developed. Discharge behaviour is not characteristic to arc discharge and, therefore, implies less destructive influence on the electrodes. The system produces non-isothermal plasma torch at atmospheric pressure, which mainly consists of active species that are beneficial for the chemical reactions.

Acknowledgements

This research has been partially supported by the Ministry of Education and Science of Ukraine, National Academy of Sciences of Ukraine, and Taras Shevchenko National University of Kyiv.

REFERENCES

[1] Prysiazhnevych I V, Chernyak V Ya, Yukhymenko V V, Naumov V V, Matejčik Š, Skalny J D, Sabo M, Ukr J Phys 52 (2007) 1061-1067.

[2] Czernichowski A, Pure Appl Chem 66 (1994) 1301-1310.

[3] Fridman A, Nester S, Kennedy L A, Saveliev A, Mutaf-Yardimci O, Prog Energy Comb Sci 25 (1999) 211-231.

[4] Bo Z, Yan J, Li X, Chi Y, Cen K, Int J Hydrogen Energy 33 (2009) 5545-5553.

[5] Sun Z W, Zhu J J, Li Z S, Alden M, Leipold F, Salewski M, Kusano Y, Optics Express 21 (2013) 6028-6044.

[6] Kalra C S, Gutsol A F, Fridmamn A A, IEEE Trans Plasma Sci 33 (2005) 32-41.

[7] Czernichowski A, In: 19th Int Symp Plasma Chem. Bochum, Germany, 2009.

[8] Cormier J-M, Rusu I, J Phys D Appl Phys 34 (2001) 2798–2803.

[9] Du C, Li H, Zhang L, Wang J, Huang D, Xiao M, Cai J, Chen Y, Yan H, Xiong Y, Xiong Y, Int J Hydrogen Energy 37 (2012) 8318-8329.

[10] Cormier J-M, Rusu I, Khacef A, In: 16th Int Symp Plasma Chem. Taormina, 2003.

[11] Solomenko O V, Nedybaliuk O A, Chernyak V Ya, Martysh E V, Fedirchyk I I, Prysiazhnevych I V, Probl At Sci Technol. Series: Plasma Electron New Accel Method 8 (2013) 213-216.

[12] Nedybaliuk O A, Chernyak V Ya, Martysh E V, Lisitchenko T E, Vergun O Yu, Orlovska S G, Probl At Sci Technol. Series: Plasma Phys 19 (2013) 219-221.
[13] Koroteev A S, Mironov V M, Svirchyk Yu S, Plasmatrons: constructions, characteristics, calculation, Mashinostrojenie, Moscow, 1993.
[14] Kalra C S, Kossitsyn M, Iskenderova K, Chirokov A, Cho Y I, Gutsol A, Fridman A, In: Electron Proc 16th Int Symp Plasma Chem. Taormina, 2003.
[15] Nedybaliuk O A, Chenyak V Ya, Olszewski S V, Martysh E V, Int J Plasma Environ Sci Technol 5 (2011) 20-24.
[16] Nedybaliuk O A, Solomenko O V, Chernyak V Ya, Martysh E V, Lisitchenko T E, Simonchik L V, Arkhipenko V I, Kirillov A A, Liptuga A I, Belenok N V, Probl At Sci Technol. Series: Plasma Phys 18 (2012) 178-180.
[17] Laux C O, Spence T G, Kruger C H, Zare R N, Plasma Source Sci Technol 12 (2003) 125-138.